

NUMERICAL STUDY OF THE MIXED CONVECTION HEAT TRANSFER IN ANNULUS HEATED BY JOULEAN EFFECT

S. Touahri and T. Boufendi

Physic Energetic Laboratory, Department of Physic, Mentouri University; Constantine; Algeria

E-mail: Sofianetouahri04@yahoo.fr

Reçu le 12/05/2014 – Accepté le 24/06/2014

Abstract

In the present work, we numerically study the three-dimensional mixed convection heat transfer in the annular space between two concentric horizontal pipes, the external pipe is heated by an electrical intensity passing through its small thickness while the inner cylinder is insulated. The convection in the fluid domain is conjugated to thermal conduction in the pipes solid thickness. The physical properties of the fluid are thermal dependant. The heat losses from the external outside pipe surface to the surrounding ambient are considered. The model equations of continuity, momenta and energy are numerically solved by a finite volume method with a second order spatiotemporal discretization. The obtained results show the three dimensional aspect of the thermal and dynamical fields with considerable variations of the viscosity and moderate variations of the fluid thermal conductivity. As expected, the mixed convection Nusselt number becomes more superior to that of the forced convection when the Grashof number is increased. At the solid-fluid interface, the results show clearly the azimuthal and axial variations of the local heat flux and the local Nusselt numbers. Following these results, we have tried modelling the average Nusselt number Nu_A as a function of Richardson number Ri . With the parameters used, the heat transfer is quantified by the correlation: $Nu_A = 9.9130 Ri^{0.0816}$.

Keywords: Mixed Convection, Annulus, Conjugate Heat Transfer, Numerical simulation.

Résumé

Dans le présent travail, on étudie numériquement le transfert de chaleur conjugué tridimensionnel dans un espace annulaire compris entre deux cylindriques concentriques horizontaux, dont le cylindre extérieur est soumis à une production d'énergie interne générée par effet Joule à travers son épaisseur tandis que celui intérieur est adiabatique. La convection thermique dans le domaine fluide est conjuguée à une conduction thermique dans le solide. Les propriétés physiques du fluide sont thermo-dépendantes et les pertes thermiques vers le milieu externe seront prises en compte. Les équations modélisantes de continuité, de mouvement et de l'énergie sont numériquement résolues par la méthode des volumes finis avec une discrétisation spatiotemporelle du second ordre. Les résultats obtenus montrent l'aspect tridimensionnel des champs thermiques et dynamiques avec des variations considérables de la viscosité et des variations modérées de la conductivité thermique du fluide. Comme prévu, le nombre de Nusselt de la convection mixte devient supérieur à celui de la convection forcée lorsque le nombre de Grashof est augmenté. Les résultats à l'interface solide-fluide du cylindre externe montrent clairement les variations azimutales et axiales du flux de chaleur local et du nombre de Nusselt local. Suite à ces résultats, nous avons essayé de modéliser le nombre de Nusselt moyen en fonction de nombre de Richardson. On trouve que la corrélation $Nu_A = 9.9130 Ri^{0.0816}$ modélise les résultats avec les conditions et les paramètres de cette étude.

Mots clés : Convection mixte, Espace annulaire, Transfert de chaleur conjugué, Simulation numérique.

ملخص

في هذا العمل المنجز، ندرس رقمياً التبادل الحراري الثلاثي الأبعاد بالحمل المختلط الرقائقي، ما بين قناتين أسطوانيتين أفقيتين متمركزتين ذات سمك ضعيف، القناة الخارجية مسخنة بتيار كهربائي عابر خلال هذا السمك، في حين أن القناة الداخلية كظومة الحمل المختلط في المائع مرافق للتوصيل الحراري في جدران القناة. الخواص الفيزيائية للمائع متعلقة بدرجة الحرارة، والضياع الحراري لجدار القناة الخارجية باتجاه الوسط الخارجي غير مهم. معادلات الإنحفاظ النموذجية للكثافة، الحركة والطاقة تحل عددياً بطريقة الحجم المنتهية وباستعمال التقسيمات في الزمن والمكان من الدرجة الثانية. النتائج المتحصل عليها تبين المظهر الثلاثي الأبعاد للحرارة والحركة مع تغيرات معتبرة في اللزوجة وتغيرات أقل اعتباراً في الناقلية الحرارية للمائع. عدد نوسالت (Nu) للحمل المختلط يصبح أكبر من عدد نوسالت للحمل القسري عند رفع عدد غراشوف. النتائج على السطح الفاصل بين المائع وجدار القناة الخارجية تبين بوضوح التغيرات الزاوية والمحورية للتدفق الحراري المحلي و عدد نوسالت المحلي. تبعاً لهذه النتائج، حاولنا إيجاد علاقة تربط بين عدد نوسالت المتوسط و عدد ريشاردسون (Ri). نجد أن العلاقة $Nu_A = 9.9130 Ri^{0.0816}$ هي التي تربط بين النتائج المتحصل عليها ومعطيات و شروط هذه الدراسة.

الكلمات المفتاحية : الحمل المختلط الرقائقي، قناتين متمركزتين، تبادل حراري مرافق، دراسة رقمية.

I. NOMENCLATURE

D_{1i}	Internal diameter of inner pipe, [m].
D_{1o}	External diameter of inner pipe, [m].
D_{2i}	Internal diameter of outer pipe, [m].
D_{2o}	External diameter of outer pipe, [m].
D_h	Hydraulic diameter, [m].
I	Electrical intensities, [A].
L	Pipe length, [m].
g	Gravitational acceleration, ($= 9.81$), [$m \cdot s^{-2}$]
G	Volumetric heat generation, [Wm^{-3}]
G^*	Non-dimensional volumetric heat generation, ($K_s^* / Re_0 Pr_0$).
Gr^*	Modified Grashof number, ($= g\beta GD_i^5 / K_s \nu^2$)
h_r	Radiative heat transfer coefficient, [$W/m^2 \cdot ^\circ K$].
h_c	Convective heat transfer coefficient, [$W/m^2 \cdot ^\circ K$].
K^*	Nondimensional thermal conductivity, (K/K_0).
K_0	Fluid thermal conductivity at the entrance, [$W/m \cdot ^\circ K$].
K_s	Pipe thermal conductivity, [$W/m \cdot ^\circ K$].
Nu	(θ, Z^*) Local Nusselt number.
Nu	(Z^*) Axial Nusselt number.
Nu_A	Average Nusselt number.
P	Pressure, [N/m^2].
P^*	Nondimensional pressure, ($(P - P_0) / \rho_0 V_0^2$).
Pr	Prandtl number, (ν/α).
r^*	Nondimensional radial coordinate.
Re	Reynolds number, ($V_0 D_h / \nu_0$).
Ri	Richardson number, (Gr/Re^2).
t^*	Nondimensional time, ($V_0 t / D_h$).
T^*	Nondimensional Temperature, ($(T - T_0) / (G D_h^2 / K_s)$).
V_0	Axial mean velocity at the entrance, [m/s].
V_θ^*	Nondimensional circumferential velocity component, (V_θ / V_0).
V_r^*	Nondimensional radial velocity component, (V_r / V_0).
V_z^*	Nondimensional axial Velocity component, (V_z / V_0).
z^*	Nondimensional axial coordinate, (z / D_h).
Greek symbols	
α	Thermal diffusivity, [$m^2 \cdot s^{-1}$]
β	Thermal expansion coefficient, [K^{-1}]
ε	Emissivity coefficient
μ	Dynamic viscosity, [$kg \cdot m \cdot s^{-1}$]

μ^*	Non-dimensional dynamic viscosity ($= \mu / \mu_0$)
ν	Kinematic viscosity, [$m^2 \cdot s^{-1}$]
θ	Angular coordinate, [rad]
ρ	Density, [$kg \cdot m^{-3}$]
σ	Stephan-Boltzmann constant ($= 5.67 \cdot 10^{-8}$), [$W \cdot m^{-2} \cdot K^{-4}$]
τ	Stress, [$N \cdot m^{-2}$]
τ^*	Non-dimensional stress ($= \tau / (\mu_0 V_0 / D_i)$)

II. INTRODUCTION

Laminar mixed convection between two concentric pipes has been studied by several workers. Nguyen et al. [1], studied theoretically the water flow in a concentric annulus, the surfaces of the system are considered is other mal and the pressure gradient along the annulus is constant. The governing system of equations is solved by the finite difference method. The results are obtained from a water temperature between 0 and 150°C, this temperature range corresponds to a Prandtl number between 1 and 14. The author has shown that the axial flow is influenced by the natural convection, thereby changing the axisymmetric shape of the velocity field and temperature. The effect of the Prandtl number of the axial flow is presented for the case of $Ra=104$ and a radius ratio $Re/Ri=2$. The obtained results show that the increasing of the Prandtl number make the axial velocity fields close to that of the forced convection. A good agreement is obtained with existing experimental and numerical results. Kotake et al [2], studied numerically the same problem, two different boundary conditions: a constant heat flux, constant temperature of the outer wall. The numerical results of average Nusselt number is in good agreement with other experimental results. Similar works has been done numerically by Kumar [3], and Chung et al. [4], Nouar [5], where the ratio D_o/D_i was considered. In the work of Habib et al [6], the inner cylinder subjected to a non-uniform heat flux, while the outer surface is adiabatic, the change in axial Nusselt number in this work is in good agreement that of a numerical study under the same condition.

Experimentally, the heat transfer by mixed convection in an annulus was studied by Mohammed et al [7], the two concentric cylinders are made of steel, $D_o/D_i = 2$, the inner tube subjected to constant heat flux, the outer tube is adiabatic, the Reynolds number is varied from 200 to 1000, while the Grashof number variation is between $6.2 \cdot 10^5$ and $1.2 \cdot 10^7$, the results show that the average Nusselt number can be linked with different dimensionless numbers by the correlation:

$$Nu_m = 2.964 (Gr \cdot Pr / Re)^{0.0326}$$

In this work, we studied numerically the heat transfer by mixed convection in an annulus between

two concentric cylinders, the physical properties of the fluid are thermo- dependent and the heat losses with the external environment are considered. The objective of our study is the correlation of average Nusselt numbers and Richardson.

III. THE GEOMETRY AND MATHEMATICAL MODEL

Fig.1 illustrates the problem geometry. We consider a long two horizontal concentric pipes having a length $L = 1$ m. The internal pipe with an inside diameter $D_{1i} = 0.96$ cm and an external diameter $D_{1o} = 1$ cm, the external pipe with an inside diameter $D_{2i} = 2$ cm and an external diameter $D_{2o} = 2.04$ cm. The hydraulic diameter $D_h = D_{2i} - D_{1o} = 1$ cm. The pipes are made of Inconel having a thermal conductivity $K_s = 20$ W/m $^\circ$ K.

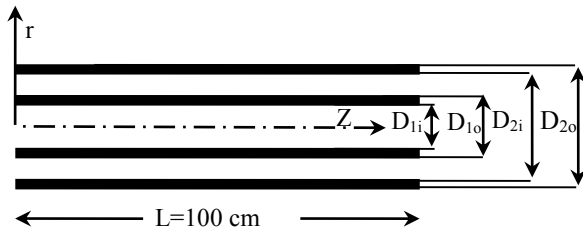


Fig. 1 Geometry of the Problem

The passing of an electrical intensity along the thickness of external pipe produced a generation of heat by the Joule effect, the considered electrical intensity values are: $I = 40, 45, 50, 55, 60$ and 65 Amperes. This heat is transferred to laminar incompressible flow of distilled water with an average velocity equal to $5.69 \cdot 10^{-2}$ m/s in the annulus. The inside surface of internal pipe is insulated, at the outer surface of external pipe, the heat losses by radiation and natural convection to the surrounding air are taken into account. At the annulus entrance, we have a uniform temperature equal to 288 K, the Reynolds number Re is equal to 500 , the Prandtl number Pr equal to 8.082 and the Grashof numbers Gr correspond to the electrical intensities are: $55734, 70538, 87084, 105372, 125401,$ and 147173 , respectively. The non-dimensional fluid viscosity and thermal conductivity variation with temperature are represented by the functions $\mu^*(T^*)$ and $K^*(T^*)$ obtained by smooth fittings of the tabulated values cited by Baehr and Stephan [8]. The combined heat transfer in the solid and fluid domains is a conjugate heat transfer problem. The physical principles involved in this problem are well modelled by the following non dimensional conservation partial differential equations with their initial and boundary conditions:

A. Modelling Equations

$$\text{At } t^* = 0, \quad V_r^* = V_\theta^* = V_z^* = T^* = 0 \quad (1)$$

At $t^* > 0$,

1) Mass Conservation Equation

$$\frac{1}{r^*} \frac{\partial}{\partial r^*} (r^* V_r^*) + \frac{1}{r^*} \frac{\partial V_\theta^*}{\partial \theta} + \frac{\partial V_z^*}{\partial z^*} = 0 \quad (2)$$

2) Radial Momentum Conservation Equation

$$\begin{aligned} \frac{\partial V_r^*}{\partial t^*} + \frac{1}{r^*} \frac{\partial}{\partial r^*} (r^* V_r^* V_r^*) + \frac{1}{r^*} \frac{\partial}{\partial \theta} (V_\theta^* V_r^*) + \\ \frac{\partial}{\partial z^*} (V_z^* V_r^*) - \frac{V_\theta^{*2}}{r^*} = - \frac{\partial P^*}{\partial r^*} + \frac{G_\theta^*}{Re_0^2} \cos \theta T^* + \\ \frac{1}{Re_0} \left[\frac{1}{r^*} \frac{\partial}{\partial r^*} (r^* \tau_{rr}^*) + \frac{1}{r^*} \frac{\partial}{\partial \theta} (\tau_{r\theta}^*) - \frac{\tau_{\theta\theta}^*}{r^*} + \frac{\partial}{\partial z^*} (\tau_{rz}^*) \right] \end{aligned} \quad (3)$$

3) Angular Momentum Conservation Equation

$$\begin{aligned} \frac{\partial V_\theta^*}{\partial t^*} + \frac{1}{r^*} \frac{\partial}{\partial r^*} (r^* V_r^* V_\theta^*) + \frac{1}{r^*} \frac{\partial}{\partial \theta} (V_\theta^* V_\theta^*) + \\ \frac{\partial}{\partial z^*} (V_z^* V_\theta^*) + \frac{V_r^* V_\theta^*}{r^*} = - \frac{1}{r^*} \frac{\partial P^*}{\partial \theta} - \\ \frac{G_\theta^*}{Re_0^2} \sin \theta T^* + \frac{1}{Re_0} \left[\frac{1}{r^{*2}} \frac{\partial}{\partial r^*} (r^{*2} \tau_{\theta r}^*) + \right. \\ \left. \frac{1}{r^*} \frac{\partial}{\partial \theta} (\tau_{\theta\theta}^*) + \frac{\partial}{\partial z^*} (\tau_{\theta z}^*) \right] \end{aligned} \quad (4)$$

4) Axial Momentum Conservation Equation

$$\begin{aligned} \frac{\partial V_z^*}{\partial t^*} + \frac{1}{r^*} \frac{\partial}{\partial r^*} (r^* V_r^* V_z^*) + \frac{1}{r^*} \frac{\partial}{\partial \theta} (V_\theta^* V_z^*) + \\ \frac{\partial}{\partial z^*} (V_z^* V_z^*) = - \frac{\partial P^*}{\partial z^*} + \\ \frac{1}{Re_0} \left[\frac{1}{r^*} \frac{\partial}{\partial r^*} (r^* \tau_{rz}^*) + \frac{1}{r^*} \frac{\partial}{\partial \theta} (\tau_{\theta z}^*) + \frac{\partial}{\partial z^*} (\tau_{zz}^*) \right] \end{aligned} \quad (5)$$

5) Energy Conservation Equation

$$\begin{aligned} \frac{\partial T^*}{\partial t^*} + \frac{1}{r^*} \frac{\partial}{\partial r^*} (r^* V_r^* T^*) + \frac{1}{r^*} \frac{\partial}{\partial \theta} (V_\theta^* T^*) + \\ \frac{\partial}{\partial z^*} (V_z^* T^*) = G^* - \\ \frac{1}{Re_0 Pr_0} \left[\frac{1}{r^*} \frac{\partial}{\partial r^*} (r^* q_r^*) + \right. \\ \left. \frac{1}{r^*} \frac{\partial}{\partial \theta} (q_\theta^*) + \frac{\partial}{\partial z^*} (q_z^*) \right] \end{aligned} \quad (6)$$

Where $G^* = \begin{cases} K_s / (Re_0 Pr_0) & \text{in the solid} \\ 0 & \text{in the fluid} \end{cases}$

The viscous stress tensor components are:

$$\begin{aligned} \tau_{rr}^* = 2\mu^* \frac{\partial V_r^*}{\partial r^*}, \quad \tau_{r\theta}^* = \tau_{\theta r}^* = \mu^* \left[r^* \frac{\partial}{\partial r^*} \left(\frac{V_\theta^*}{r^*} \right) + \frac{1}{r^*} \frac{\partial V_r^*}{\partial \theta} \right] \\ \tau_{\theta\theta}^* = 2\mu^* \left[\frac{1}{r^*} \frac{\partial V_\theta^*}{\partial \theta} + \frac{V_r^*}{r^*} \right], \quad \tau_{\theta z}^* = \tau_{z\theta}^* = \mu^* \left[\frac{\partial V_\theta^*}{\partial z^*} + \frac{1}{r^*} \frac{\partial V_z^*}{\partial \theta} \right] \\ \tau_{zz}^* = 2\mu^* \frac{\partial V_z^*}{\partial z^*}, \quad \tau_{zr}^* = \tau_{rz}^* = \mu^* \left[\frac{\partial V_z^*}{\partial r^*} + \frac{1}{r^*} \frac{\partial V_r^*}{\partial z^*} \right] \end{aligned} \quad (7)$$

The heat fluxes are:

$$q_r^* = -K^* \frac{\partial T^*}{\partial r^*}, \quad q_\theta^* = -\frac{K^*}{r^*} \frac{\partial T^*}{\partial \theta} \quad \text{and} \quad q_z^* = -K^* \frac{\partial T^*}{\partial z^*} \quad (8)$$

B. The Boundary Conditions

1) At the Annulus Entrance : $Z^*=0$

In the Fluid Domain: $0.5435 \leq r^ \leq 1.0435$ and $0 \leq \theta \leq 2\pi$

$$V_r^* = V_\theta^* = T^* = 0, V_z^* = 1 \quad (9)$$

*In the Solid Domain:

$0.5 \leq r^* \leq 0.5435$ or $1.0435 \leq r^* \leq 1.0870$ and $0 \leq \theta \leq 2\pi$

$$V_r^* = V_\theta^* = V_z^* = T^* = 0 \quad (10)$$

2) At the Annulus Exit : $Z^*=217.39$

In the Fluid Domain: $0.5435 \leq r^ \leq 1.0435$ and $0 \leq \theta \leq 2\pi$

$$\frac{\partial V_r^*}{\partial z^*} = \frac{\partial V_\theta^*}{\partial z^*} = \frac{\partial V_z^*}{\partial z^*} = \frac{\partial}{\partial z^*} \left(K^* \frac{\partial T^*}{\partial z^*} \right) = 0 \quad (11)$$

*In the Solid Domain:

$0.5 \leq r^* \leq 0.5435$ or $1.0435 \leq r^* \leq 1.0870$ and $0 \leq \theta \leq 2\pi$

$$V_r^* = V_\theta^* = V_z^* = \frac{\partial}{\partial z^*} \left(K^* \frac{\partial T^*}{\partial z^*} \right) = 0 \quad (12)$$

3) At the Inside Wall of Internal Pipe: $r^*=0.5$

$$V_r^* = V_\theta^* = V_z^* = 0 \quad \text{and} \quad \frac{\partial T^*}{\partial r^*} = 0 \quad (13)$$

4) At the Outer Wall of External Pipe: $r^*=1.0870$

$$\begin{cases} V_r^* = V_\theta^* = V_z^* = 0 \\ -K^* \frac{\partial T^*}{\partial r^*} = \frac{(h_r + h_c) D_i}{K_0} T^* \end{cases} \quad (14)$$

$$h_r = \varepsilon \sigma (T^2 + T_\infty^2)(T + T_\infty) \quad (15)$$

The emissivity of the outer wall ε is arbitrarily chosen to 0.9 while h_c is derived from the correlation of Churchill and Chu [9] valid for all Pr and for Rayleigh numbers in the range $10^{-6} \leq Ra \leq 10^9$.

$$\begin{aligned} Nu &= [h_c D_i / K_{aw}] \\ &= \left[0.6 + \left(0.387 Ra^{1/6} / \left(1 + (0.559 / Pr_{aw})^{9/16} \right)^{8/27} \right)^2 \right] \end{aligned} \quad (16)$$

C. Nusselt Number

At the solid-fluid interface ($r^*=1.0435$) the local Nusselt number is defined as:

$$Nu(\theta, Z^*) = \frac{h(\theta, Z^*) D}{k} = \frac{1}{[T^*(r^*, \theta, z^*) - T_\infty^*(z^*)]} \quad (17)$$

The axial Nusselt number is defined as:

$$Nu(z^*) = \frac{1}{2\pi} \int_0^{2\pi} Nu(\theta, z^*) d\theta \quad (18)$$

The average Nusselt number for the whole solid-fluid interface is defined as:

$$Nu_A = \frac{1}{(2\pi)(217.39)} \int_0^{2\pi} \int_0^{217.39} Nu(\theta, z^*) dz^* d\theta \quad (19)$$

IV. THE NUMERICAL METHOD

For the numerical solution of modelling equations, we used the finite volume method well described by Patankar [10]. The using of this method involves the

discretization of the physical domain into a discrete domain constituted of finite volumes where the modelling equations are discretized in a typical volume. We used a temporal discretization with a truncation error of $(\Delta t^*)^2$ order. The mesh used contains $26 \times 44 \times 162$ points in the radial, azimuthal and axial directions. The considered time step is $\Delta t^* = 5 \cdot 10^{-4}$. The accuracy of the results of our numerical code has been tested by the comparison of our results with those of Nouar[11] who studied numerically the effect of the dynamic viscosity of the mixed convection between two concentric horizontal pipes. The inner cylinder and the outer cylinder are subjected to a constant heat flux. The controlling parameters of the problem are: $Re = 35$, $Pr = 557.3$, $Gr = 6000$, $L/D_h = 125$. In Fig. 2 we illustrate the axial temperature variation at the top ($\theta = 0$) and bottom ($\theta = \pi$) of the external interface (fluid-outer pipe).

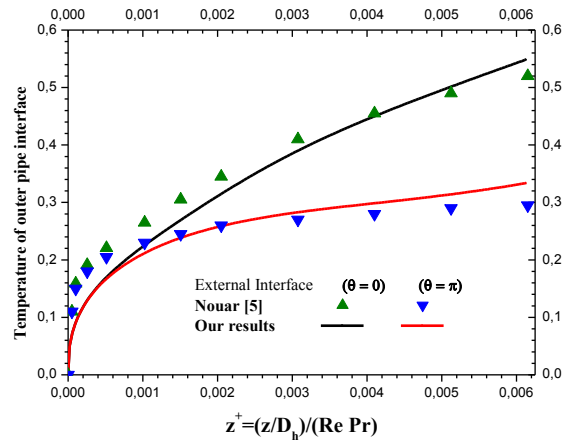


Fig. 2 Axial Evolution of the interface temperature (fluid-Outer pipe); a Comparison with the Results of Nouar[5].

It is seen that there is a good agreement between our results and theirs.

V. RESULTS AND DISCUSSIONS

A. Development of the Secondary Flow

The obtained flow for the considered cases is characterized by a main flow in the axial direction and a secondary flow in the (r^*, θ) plan. Qualitatively we note the similarity of results for the six study cases. Quantitatively, the effect of mixed convection becomes increasingly important with the increase of volumetric heating. For this, the figures presented are those of the higher volumetric heating, case of $Gr = 147173$. In fig. 3, we present the secondary flow at the annulus exit ($Z^*=100$). The transverse movement is explained as follows: the hot fluid moves

along the hot wall from the bottom of the outer tube ($\theta=\pi$) upwards ($\theta=0$) and moves down from the top to the bottom along the inner tube. The vertical plane passing through the angles ($\theta=0$) and ($\theta=\pi$) is a plane of symmetry.

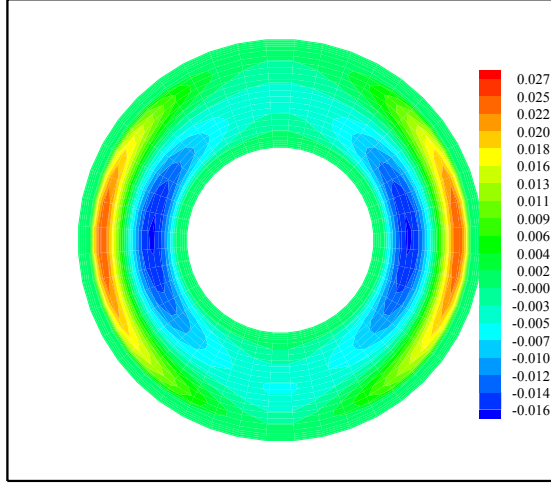


Fig. 3 Secondary Flow at the Exit of the Annulus for $Gr=147173$

The transverse flow in the (r^*, θ) plane is represented by two similar but counter rotating cells. We noticed that the centre of the rotating cells moves downward continuously along the axial direction.

B. Development of the Axial Flow

At the entrance, the axial flow is axisymmetric, after this latter is influenced by the transverse movement of the fluid. The maximum axial velocity is all the time at the top of the annulus because the fluid viscosity decreased from bottom to top. In fig.4, we present the axial flow distribution at the exit of the annulus.

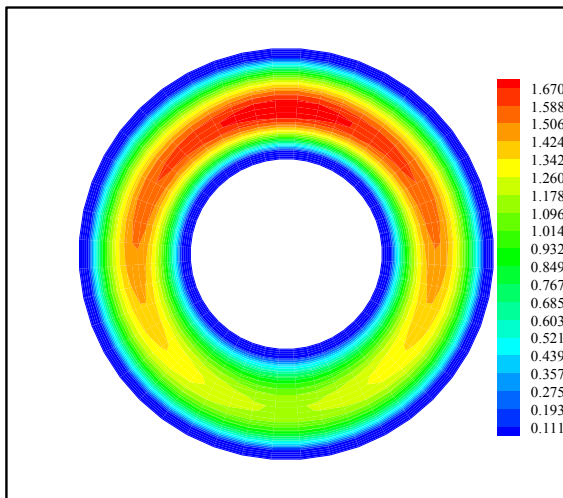


Fig. 4 Axial Velocity Profiles at the Exit of the Annulus for $Gr=147173$

C. Development of the Temperature Field

In the reference case (forced convection), the distribution of the fluid temperature in the absence of transverse motion is axisymmetric. For a given section, the isotherms are concentric circles with a maximum temperature on the inner wall of the external cylinder and a minimum temperature on the outer wall of the internal cylinder. In the presence of volumetric heating, a transverse flow exists and thus changes the axisymmetric distribution of fluid and pipe wall temperature and gives it an angular variation, this variation explained as follows: the hot fluid near the hot pipe wall moves upwards under the buoyancy force effect, the relatively cold fluid descends down near the internal pipe. This movement of the secondary flow is the cause of the azimuthally temperature variation. The obtained results show that at given section, the maximum temperature T^* is all the time located at $r^*=1$ and $\theta=0$ (top of solid-fluid interface), because the hot fluid is driven by the secondary motion towards the top of the annulus. The minimum temperature is within the core fluid, in the lower part of the annulus at $\theta=\pi$. In fig. 5, we present the polar temperature distribution at the exit of the annulus for $Gr=147173$.

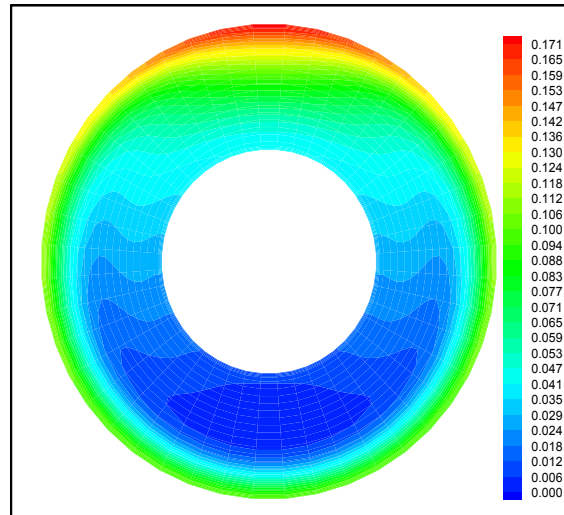


Fig. 5 The Isotherms at the Exit of the Annulus for $Gr=147173$

D. The Nusselt numbers

The phenomenon of heat transfer has been characterised in terms of circumferentially Nusselt numbers calculated at the inner wall of external pipe, which is obtained by (19). The variation of local Nusselt number of the solid-fluid interface is presented in fig. 8 for $Gr=147173$. From the entrance to the exit, we notice the large axial and angular variations of local Nusselt numbers, it takes a minimum value at ($\theta=0$) and maximum value at ($\theta=\pi$).

Fig. 9 shows the axial variation of Nusselt number for the seven studied cases. At the zone of entrance, the axial Nusselt number decreases rapidly for all studied cases. After, it increases and takes maximum value at the exit of annulus equal to: 7.58, 7.96, 8.35, 8.74, 9.06

and 9.45 for $Gr = 55734, 70538, 87084, 105372, 125401, \text{ and } 147173$ respectively. The axial Nusselt numbers increases with the increase of volumetric heating.

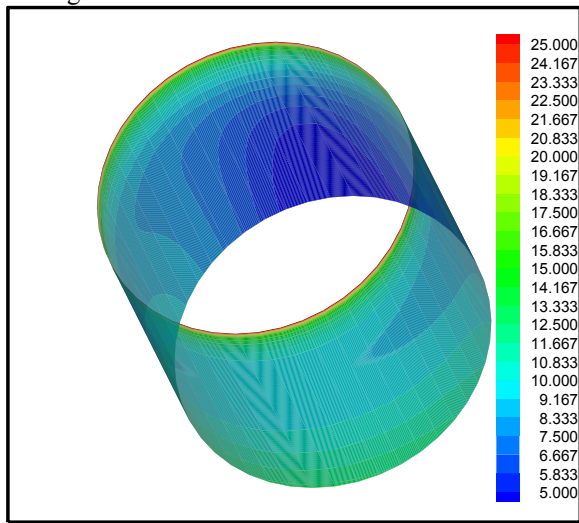


Fig. 8 The Local Nusselt Number Variation for $Gr = 147173$.

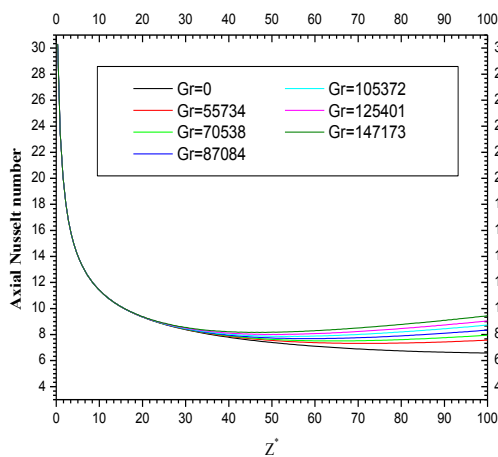


Fig. 9 The Axial Nusselt Number Variation for Different Grashof Numbers

In Tab. 1 we present the average Nusselt numbers of all studied cases:

TABLE I. Average Nusselt Numbers

Gr	55734	70538	87084	105372	125401	147173
Ri	0.223	0.282	0.348	0.421	0.502	0.589
Nu_A	8.803	8.928	9.068	9.220	9.359	9.529

The results obtained allowed us to model the average Nusselt number of the mixed convection in function of Richardson number, we found that the results with the parameters used are correlated with the correlation:

$$Nu_A = 9.9130 Ri^{0.0816} (22)$$

VI. CONCLUSION

This study considers the numerical simulation of the three dimensional mixed convection heat transfer in horizontal annulus, the external pipe is heated by an electrical intensity passing through its small thickness and the internal pipe is insulated. The obtained results show that:

- * The dynamic and thermal fields for mixed convection are qualitatively and quantitatively different from those of forced convection.

- * Although the volumetric heat input in the solid thickness is constant, the heat flux at the solid-fluid interface is not constant: it varies with θ and z , that is a characteristic of the considered mixed convection.

- * The azimuthally variation of temperature at a given section is important; this phenomenon is demonstrated by the circumferential temperature variation of the wall. There is a large temperature wall difference between top and bottom of the external pipe.

- * The physical properties are thermo-dependent (the dimensionless dynamic viscosity varies from 1.018 at the entrance to 0.4171 at the exit).

- * For the forced convection, the average Nusselt number is 8.803. Thus, for the mixed convection, the parameters used are well correlated with the correlation: $Nu_A = 9.9130 Ri^{0.0816}$.

VII. REFERENCES

- [1] T.H. Nguyen, P. Vasseur, L. Robillard, B. Shekhar, "Combined free and forced convection of water between horizontal concentric annuli", *J. Heat Transfer*, Vol. 105, 1983, pp.498-504.
- [2] S. Kotake, N. Hattori, "Combined forced and free convection heat transfer for fully-developed laminar flow in horizontal annuli", *Int. J. Heat Mass Transfer*, vol. 28, 1985, pp. 2113-2120.
- [3] R. Kumar, "Study of natural convection in horizontal annuli", *Int. J. Heat Mass Transfer*, vol. 31, 1988, pp. 1137-1148.
- [4] S. Y. Chung, G. H. Rhee, et H. J. Sung, "Direct Numerical Simulation of Concentric Annular Pipe Flow" *Part I: Flow Field*, *Int. J. Heat Fluid Flow*, vol. 23, 2002, pp. 426-440.
- [5] C. NOUAR, "Numerical solution for laminar mixed convection in a horizontal annular duct: temperature-dependent viscosity effect", *Int. J. Numer. Meth. Fluids* Vol. 29, 1999, pp. 849-864.
- [6] M. A. Habib, A. A. A. Negm, "Laminar mixed convection in horizontal concentric annuli with non-uniform circumferential heating" , *Int. J. Heat Fluid Flow*, Vol. 37, 2001, pp. 427-435.
- [7] H.A. Mohammed, Antonio Campo, R. Saidur, "Experimental study of forced and free convective heat transfer in the thermal entry region of horizontal concentric annuli",

- International Communications in Heat and Mass Transfer*, Vol. 37, 2010, pp. 739–747.
- [8] H.D. Baehr and K. Stephan, *Heat and Mass Transfer*, Transl. by N. JanePark, p. 619, pringer-Verlag, Berlin: 1998.
- [9] S.W. Churchill, H.S. Chu, "Correlating Equation for Laminar and Turbulent Free Convection from a Horizontal Cylinder", *International Journal of Heat and Mass Transfer*, Vol 18, 1975, pp. 1049-1053
- [10] S.V. Patankar, *Numerical Heat Transfer and Fluid Flow*, McGraw-Hill, New-York: 1980.

